土木学会論文集 A2（応用力学）, Vol. 70, No. 2（応用力学論文集 Vol. 17）, I_743-I_752, 2014.

The Effects of Surface Charging Properties on Colloid Transport in Porous Media

Motoyoshi KOBAYASHI[1], Masaru OOKAWA[2] and Shouichi YAMADA[2]

[1]Member of JSCE, Associate Professor, Faculty of Life and Environmental Sciences, University of Tsukuba
(1-1-1 Tennodai, Tsukuba, Ibaraki 305-8572, Japan)
E-mail:kobayashi.moto.fp@u.tsukuba.ac.jp
[2]Former Student at Faculty of Agriculture, Iwate University
(3-18-8 Ueda, Morioka, Iwate 020-8550, Japan)

Transport properties of colloidal particles in a packed bed of collector beads are affected by hydrodynamic and colloidal interactions between particles as well as between the particle and the collector. The colloidal interaction depends on the surface charging of collectors and particles. While many researchers have studied on the colloid deposition and transport in porous media as a function of ionic strength, experimental investigations examining the effect of surface charge are scarce. To figure out the effect of surface charge on the colloid transport in porous media, we have performed colloid transport experiments in a packed bed of spherical beads. In the present experiment, we used sulfate latex with a constant negative charge and carboxylate latex having pH-dependent negative charge as colloidal particles. Zirconia beads with pH-dependent charge and an isoelectric point around pH 7 were adopted as collectors. Colloid transport experiments were carried out in 1 mM KCl as a function of pH and breakthrough curves of colloid were obtained. The experimental breakthrough curves were analyzed by a convection-dispersion equation including colloid deposition, where colloid filtration and dynamic blocking are considered. The results of experiments and analysis show that the maximum surface coverage of sulfate latex on the collector surface is constant against pH change. On the one hand, the maximum coverage of carboxyl latex decreases with increasing pH, indicating that the lateral particle-particle repulsion increased by high charge enhances blocking in later stage of deposition. The result suggests that electro-hydrodynamic interaction also affects the maximum coverage.

Key Words: *blocking, deposition, zirconia, latex, electrostatic interaction*

1. INTRODUCTION

Transport of colloidal particles in porous media is important in many industrial and environmental fields, e.g., contaminants transport in subsurface environments and deep bed filtration in solid-liquid separation etc.[1),2),3),4),5)]. Transport behaviors of colloidal particles in porous media are reflected by the hydrodynamic and colloidal interactions between particles and/or between particles and collector materials making porous media[3),4),5),6),7),8)]. For the better understanding on these interactions, many experimental and theoretical studies have been carried out for simple systems[3),4),5),6),7),8)].

Colloid transport in granular porous media depends on the kinetics of particle deposition onto the surface of collectors composing porous media. The theoretical treatment of deposition consists of the transport process of colloidal particles as well as the physicochemical interactions between particles and between particles and collectors[3),4),5),6),7),8)]. The physicochemical interactions are generally given by the Derjaguin-Landau and Verwey-Overbeek (DLVO) force, which is the superposition of electric double layer and the van der Waals forces and is influenced by the surface charge, ionic strength, and the solution pH, etc.[3),6),9)]. In the early stage of deposition, the process is determined by the collision of a colloidal particle onto a collector in porous media. So-called colloid filtration theories, based on the trajectory analysis calculating the colliding path of a colloidal particle or the convective-dispersion equation evaluating the colliding flux, have been developed[4),5)]. The colloid filtration theory evaluates the single-collector efficiency that is the ratio of the number of particles to be attached on the collector to the number of colliding particles passing through the projected area of the collector. The colloid filtration theory nowadays

takes account of the effect of surrounding collectors on flow field around a collector bead, the colloidal and hydrodynamic interactions, and Brownian diffusion.

The validity of the colloid filtration theory has been experimentally examined in many particles and model porous media[3),4),5),6)]. The results verify the usefulness of the colloid filtration theory. That is, the theory quantitatively predicts the single-collector efficiency in the absence of electrostatic force realized at high salt concentration[5),6)]. Also, the theory quantitatively works in the wide range of salt concentration when the attractive electric double layer force between oppositely charged particles and collectors is dominant[3),6)]. On the one hand, in the presence of repulsive double layer force between similarly charged surfaces, the colloid filtration theory underestimates the single collector efficiency[2),3)]. This discrepancy has been recognized as a classical shortage of the DLVO theory. Similar conclusions have been accepted for the aggregation kinetics of colloidal particles[3),10),11)].

As the deposition of stable colloidal particles onto the surface of oppositely charged collector proceeds, the collector surface is covered with deposited particles. The lateral repulsion between a depositing particle and a previously deposited particle reduces the chance of further deposition. This phenomenon is called a blocking[7),8)]. The blocking dynamics needs to be quantitatively understood to describe the colloid transport in porous media in addition to the single collector efficiency[7),8)]. Simpler model systems, the deposition and subsequent blocking on planar surfaces, have been studied as well[12),13),14),15),16)]. The outcomes from such simple systems provide important knowledge on the deposition in porous media.

Previous studies on the blocking have shown that the random sequential adsorption (RSA) is an useful model when describing the blocking process[7),12),16)]. In the RSA model, depositing particles are sequentially placed on the random position on the collector surface. The overlapping of deposited particles is not allowed on the surface. Therefore, in the later stage of deposition, the deposition is inhibited and finally no deposition can be realized. The maximum surface overage or the jamming limit by the RSA is around 0.55 (0.546 or 0.547) for the deposition of hard spheres[7),12),16)]. In the case of colloidal particles, the lateral double layer repulsion further reduces the maximum surface coverage due to the increase of the effective radius. Thus, the maximum surface coverage decreases with decreasing salt concentration due to the development of diffuse double layer[7),12),13),14)]. The RSA model with electric double layer potential successfully describes the maximum surface coverage of diffusional deposition of nanoparticles and dendritic polyelectrolytes on planar surfaces[12),13)]. Also, the maximum surface coverage in the deposition in granular porous media qualitatively follows the RSA model with double layer force in terms of the dependence of surface coverage on salt concentration[7),8)]. However, while the electric double layer force is dependent on the surface charge[3),9),10)], the effect of surface charge on the later stage of deposition has not yet been studied for the deposition in porous media of packed collector beads.

The success of the RSA model indicates that the blocking is mainly controlled not by the interaction between collector and colloidal particle but by the lateral interaction between colloidal particles. Nevertheless, in some cases, the maximum coverage is higher than that expected by the RSA with double layer force[13),14)]. This increase of the maximum coverage is attributed to the increased attractive force between the adsorbate and the collector enhanced by the highly charged surface of the collector. At this moment, however, systematic studies on such enhancement have been scarce for the deposition in granular porous media. Thus, the effect of charging of both collectors and colloidal particles on the colloid transport in porous media should be systematically examined.

In this context, to figure out the effect of surface charge on colloid transport in porous media, we have performed the experiment on the transport of colloidal sulfate or carboxyl latex particles in a packed bed of spherical zirconia beads. In the system, the sulfate latex particles have a constant negative surface charge density[17),18)] and the carboxyl latex particles bear pH-dependent negative charge[9),10)]. On the one hand, the collector beads of zirconia carry pH-dependent surface charge with an isoelectric point of pH; the zirconia is positively charged at pH < 7 and negatively charged at pH >7 [6)]. Thus, we can examine the influence of surface charge of the particles and the collector on the colloid transport in porous media by changing the solution pH. Experimental data of colloid breakthrough curve is analyzed by a convective-dispersion equation including the deposition dynamic with the single collector efficiency and the dynamic blocking function. The main focus is the pH-dependent maximum surface coverage.

2. EXPERIMENTAL METHOD

(1) Materials

We used two types of latex particles as model colloidal particles. One is sulfate latex with a diameter $2a_p$=2.0 μm and a surface charge density σ=-0.084 C/m^2. The sulfate latex particles can be considered to have a constant negative surface charge density because their surface groups are strong acid. The other

is carboxylate latex with a diameter of $2a_p$=0.51 μm and pH-dependent negative charge due to the deprotonation of carboxyl groups. The density of latex particles is 1.055 Mg/m^3. These particles were used for colloid transport and electrophoretic mobility experiments.

In colloid transport experiments in porous media, we adopted a packed bed of zirconia beads with a diameter $2a_c$=326±8 μm and a density of 6.0 Mg/m^3 in a column. The beads were washed by about 1 M NaOH, rinsed with pure water, dried, heated at 600 ℃, cooled down and stored in a polyethylene container. For the measurement of electrophoretic mobility, colloidal zirconia particles with an experimentally determined hydrodynamic diameter of 0.34 μm obtained using dynamic light scattering. The colloidal zirconia particles were purified by dialysis in a Visking tube against pure water.

Salt concentration and suspension pH were adjusted by the addition of KCl, HCl and $NaHCO_3$. All solutions and suspensions were prepared from purified deionized water.

(2) Electrophoretic mobility of colloidal particles

To characterize the surface charging behavior of used colloidal particles, we measured electrophoretic mobility of colloidal particles by using electrophoretic light scattering technique. The electrophoretic mobilities of carboxyl latex and zirconia were measured as a function of pH in 1 mM (=mmol/L) KCl. The mobility of sulfate latex was almost pH-inde pendent and was measured as a function of KCl concentration to characterize the surface charge density. The particle concentrations at measurements were 11, 135 and 31 mg/L for sulfate latex, carboxyl latex and zirconia, respectively. Samples were prepared by diluting stock suspensions by adding appropriate volumes of water, KCl solution, HCl solution or KOH solution to change pH and KCl concentration. The pH of suspensions was measured by means of a combination glass electrode. All experiments were carried out at 20˚C.

(3) Colloid transport experiment in a packed bed of zirconia beads

Experimental setup is shown in **Fig. 1**. Porous media were prepared by wet-packing of zirconia beads in an acrylic column with an inner diameter of 1.8 cm. The zirconia beads were put between two rubber stoppers covered with nylon meshes. The height L and porosity f of the packed bed were 3.1 cm and 0.37. Colloid suspension was flowed into the column through a silicone tube by using a peristaltic pump. The concentration of colloidal particles in the effluent from the column C was measured with a spectrophotometer.

The procedure of colloid transport experiments was as follows. The column was flushed with pure water, followed by background solution with various salt concentration and pH without latex particles, until the electric conductivity of effluent solution reached that of influent. The conductivity was checked with a compact conductivity meter. Then, the latex suspension with a concentration C_0=75 mg/L for sulfate latex or C_0=100 mg/L for carboxyl latex was fed into the column with a flow rate Q of 0.15 cm^3/s. The direction of flow was upward to keep saturate condition in the column. The colloid transport experiment was carried out as a function of pH at 1 mM KCl. The pH was changed by adding HCl and $NaHCO_3$. The pH of effluent suspension was measured by means of a combination glass electrode. From the experiments, colloid breakthrough curves were obtained as a function of pH. Experiments were conducted in an air-conditioned room at 20˚C.

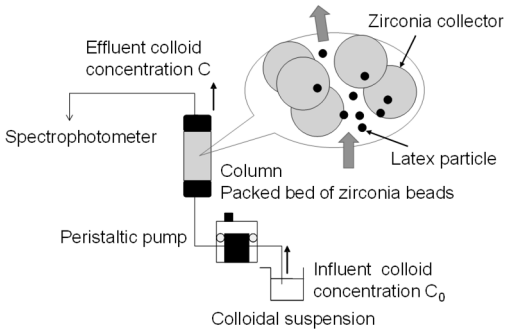

Fig.1 Schematic illustration of experimental setup.

3. THEORETICAL CALCULATION

(1) Electrophoretic mobility

Measured electrophoretic mobility was analyzed by electrokinetic and electric charging models. Ohshima and Helmholtz-Smoluchowski theories can be used to calculate electrophoretic mobility μ_m from zeta potential ζ that is the electric potential near the charged interface[3),19)]. At higher magnitude of zeta potential, the relaxation/polarization of diffuse double layer reduces electrophoretic mobility and therefore the mobility vs. zeta potential relation shows maximum/minimum[9),10),17),18),19),20)]. Such reducing effect is included in Ohshima's equation. Ohshima's equation for the electrophoretic mobility μ_m of a sphere with a radius a_p immersed in 1-1 electrolyte solution like KCl with ionic strength I is given by

$$\mu_m = \frac{2\varepsilon_r \varepsilon_0 k_B T}{3\mu e} E_m \qquad (1)$$

$$E_m = \mathrm{sgn}(\zeta)\left\{\frac{3}{2}\tilde{\zeta} - \frac{3F}{1+F}H + \frac{1}{\kappa a_p}\left[-18\left(t_\mathrm{m} + \frac{t_\mathrm{m}^3}{9}\right)K + \frac{15F}{1+F}\left(t_\mathrm{m} + \frac{7t_\mathrm{m}^2}{20} + \frac{t_\mathrm{m}^3}{9}\right) - 6(1+3\tilde{m})\left(1-\exp(-\tilde{\zeta}/2)\right)G + \frac{12F}{(1+F)^2}H + \frac{9\tilde{\zeta}}{1+F}(\tilde{m}G + mH) - \frac{36F}{1+F}\left(\tilde{m}G^2 + \frac{m}{1+F}H^2\right)\right]\right\} \quad (2)$$

$$\tilde{\zeta} = \frac{e|\zeta|}{k_B T} \quad (3)$$

$$\kappa^{-1} = \sqrt{\frac{\varepsilon_r \varepsilon_0 k_B T}{2N_A e^2 I}} \quad (4)$$

$$m = \frac{2\varepsilon_r \varepsilon_0 k_B T}{3\mu e^2}\lambda_\mathrm{i}, \quad \tilde{m} = \frac{2\varepsilon_r \varepsilon_0 k_B T}{3\mu e^2}\tilde{\lambda}_\mathrm{i} \quad (5)$$

$$\lambda_i = \frac{N_A e^2}{\Lambda_i^0} \quad (6)$$

$$F = \frac{2}{\kappa a_p}(1+3m)\left\{\exp(\tilde{\zeta}/2) - 1\right\} \quad (7)$$

$$G = \ln\left[\frac{1+\exp(-\tilde{\zeta}/2)}{2}\right] \quad (8)$$

$$H = \ln\left[\frac{1+\exp(|\tilde{\zeta}|/2)}{2}\right] \quad (9)$$

$$t_\mathrm{m} = \tanh\frac{\tilde{\zeta}}{4} \quad (10)$$

$$K = 1 - \frac{25}{3(\kappa a_p + 10)}\exp\left[-\frac{\kappa a_p}{6(\kappa a_p - 6)}\tilde{\zeta}\right] \quad (11)$$

where $\varepsilon_r\varepsilon_0$ is the permittivity of water, k_B is the Boltzmann constant, T is the absolute temperature, e is the elementary charge, μ is the viscosity of solution, N_A is Avogadro's number, κ^{-1} is the Debye length which is a measure of the thickness of diffuse double layer. Λ_i^0 is the limiting molar conductance of ith ion species; $\Lambda_\mathrm{i}^0 = 73.48\times10^{-4}$ and 76.31×10^{-4} m^2 S/mol for K^+ and Cl^- at 25 °C [21]. The values should be increased by 2 % / °C as the temperature increases from 25 °C [21]. m and $\tilde{m}$ are for the counter-ion and the co-ion, respectively. The first term of the right hand side of Eq. (2) corresponds to Helmholtz-Smoluchowski equation, which is only valid for low zeta potential and high ionic strength.

The Gouy-Chapman theory of electric diffuse double layer provides the relationship between surface charge σ and surface potential Ψ_0 written as [9),10),20)]

$$\sigma = \frac{2\varepsilon_r \varepsilon_0 k_B T \kappa}{e}\sinh\left(\frac{e\Psi_0}{2k_B T}\right). \quad (12)$$

With this equation, we can evaluate surface potential from surface charge density. Zeta potential is defined as the potential at slipping plane, within which liquid moves with the same velocity as the that of solid-liquid interface. The distance to the slipping plane from the interface x_s is around 0-1 nm [9),10)17),18)]. Zeta potential ζ can be calculated by the following equation

$$\zeta = \frac{4k_B T}{e}\mathrm{arctanh}\left[\exp(-\kappa x_s)\tanh\left(\frac{e\Psi_0}{4k_B T}\right)\right] \quad (13)$$

from the Gouy-Chapman theory[9),10),17),18)]. Using Eqs. (1), (12), and (13) we can evaluate electrophoretic mobility of sulfate latex bearing constant surface charge density.

The surface charge density of carboxyl latex and zirconia in aqueous solutions depends on the solution pH. The 1 pK Gouy-Chapman (GC) model is available to model the charging behavior of carboxyl latex[9),10)]. The charge originates from deprotonated sites on the surface carboxyl groups. Therefore,

$$\sigma = -e[\text{-COO}^-] \quad (14)$$

is given, where $[\text{-COO}^-]$ is the surface density of deprotonated carboxyl sites. The surface density of the total chargeable sites Γ_T is the sum of surface density of deprotonated and protonated sites $[\text{-COOH}]$.

$$\Gamma_\mathrm{T} = [\text{-COO}^-] + [\text{-COOH}] \quad (15)$$

The balance of these sites is controlled by the following mass action law

$$\frac{10^{-\mathrm{pH}}\exp\left(\frac{-e\Psi_0}{k_B T}\right)[-\mathrm{COO}^-]}{[-\mathrm{COOH}]} = K = 10^{-\mathrm{p}K} \quad (16)$$

where K is the proton dissociation constant reflecting the affinity of proton to the carboxyl groups. With 1pK-GC model with proper parameters Γ_T and pK,

one can calculate surface charge density and electrophoretic mobility of carboxyl latex as a function of pH. The above procedure can be used to evaluate surface potential, which is needed to evaluate interaction potential between colloidal particles.

(2) Colloid transport in porous media

Transport of colloidal particles in porous media can be described by the following convection dispersion equation including the deposition of colloidal particles onto collectors composing packed bed[7),8)]. That is, the change of colloid concentration C at position x and time t in porous media is governed by

$$\frac{\partial C}{\partial t} = D_h \frac{\partial^2 C}{\partial x^2} - v_p \frac{\partial C}{\partial x} - w\left[k_{pc} B(\theta) + k_{pp}\theta\right] C \quad (17)$$

$$B(\theta) = 1 - 4\beta\theta + \frac{6\sqrt{3}}{\pi}(\beta\theta)^2 + \left(\frac{40}{\sqrt{3}\pi} - \frac{176}{3\pi^2}\right)(\beta\theta)^3 \quad (18)$$

$$\frac{\partial \theta}{\partial t} = k_{pc} B(\theta) \pi a_p{}^2 C \quad (19)$$

The last equation describes the temporal change of the surface coverage of colloidal particles on collector θ. In Eqs. (17)-(19), $B(\theta)$ is the dynamic blocking function based on the random sequential adsorption (RSA) model describing the reduction of available area for deposition due to the increase of surface coverage, β is the blocking parameter and is related to the maximum surface coverage[7)] θ_{max} as $\beta = 0.44/\theta_{max}$, v_p is the average interstitial velocity, $D_h = \alpha_L v_p$ is the hydrodynamic dispersion coefficient and α_L is the dispersivity (here, $\alpha_L = 6.4\times10^{-4}$ m from the experiment of tracer breakthrough curve), $w = 3(1-f)/(fa_c)$ is the surface area of collector per unit pore volume, f is porosity, $k_{pc} = k^f \alpha_{pc}$ is the deposition rate of colloidal particles to collector surface, $k_{pp} = k^f \alpha_{pp}$ is the multiple deposition rate of colloidal particles to deposited particles on collector surface, α_{pc} is the capture efficiency of deposition between collector and colloidal particle, α_{pp} is the capture efficiency of colliding particles to deposited particles, $k^f = \eta U/4$ is the fast rate of deposition, U is the approach velocity of suspension to the column, η is single-collector efficiency describing the ratio of the number of particles to be attached to the number of particles passing through the projected area of a collector bead without electrostatic interaction. One can evaluate single collector efficiency η from the Tufenkji and Elimelech correlation equation[5)] that takes into account the flow field around a collector bead in porous media by using Happel's cell model and consider the particle transport by diffusion, sedimentation, and interception. Hydrodynamic and van der Waals attractive interactions are also included, but electrostatic interaction is neglected. The single collector efficiency η by Tufenkji and Elimelech is written as

$$\eta = 2.4 A_s^{\frac{1}{3}} N_R^{-0.081} N_{Pe}^{-0.715} N_{vdW}^{-0.052} + 0.55 A_s N_R^{1.675} N_A^{0.125} + 0.22 N_R^{-0.24} N_G^{1.11} N_{vdW}^{0.053} \quad (20)$$

in which non-dimensional parameters are given as follows:

$$A_s = \frac{2(1-p^5)}{2-3p+3p^5-2p^6} \quad (21)$$

$$p = (1-f)^{1/3} \quad (22)$$

$$N_R = \frac{a_p}{a_c} \quad (23)$$

$$N_{Pe} = \frac{2Ua_c \cdot 6\pi a_p \mu}{k_B T} \quad (24)$$

$$N_{vdW} = \frac{A}{k_B T} \quad (25)$$

$$N_A = \frac{A}{12\pi\mu a_p^2 U} \quad (26)$$

$$N_G = \frac{2}{9}\frac{a_p^2(\rho_p - \rho_f)g}{\mu U} \quad (27)$$

where A is the Hamaker constant being a measure for the van der Waals attractive interaction energy ($A = 4.3\times10^{-20}$ J for the interaction between zirconia and latex), g is the gravity acceleration, ρ_p and ρ_f are particle density and fluid density, respectively. In these equations, unknown parameters are α_{pc}, α_{pp}, and β.

One can describe colloid transport in porous media by numerically solving Eq. (17). We tuned unknown parameters α_{pc}, α_{pp}, and β by trial and error method to obtain the good agreement between the calculated breakthrough curve and the experimental breakthrough curve. In the present experimental conditions, we expect $\alpha_{pp} = 0$ and $\alpha_{pc} = 1$ for sulfate latex. This is because electrostatic repulsion between colloidal particles prevents aggregation and thus multiple deposition is negligible ($\alpha_{pp} = 0$). Also, the electrostatic attraction between oppositely charged colloidal particle and collector gives rise to the significant enhancement of the deposition only at very low salt concentration[3),6),22),23),24),25)]; the enhancement of

particle deposition on collector surface does not occur at 1 mM adopted in this study and thus the van der Waals force is dominant as physicochemical force (α_{pc}=1). Similar behavior is expected for carboxyl latex[9),10)] except at low pH, where multiple deposition can occur ($\alpha_{pp} > 0$) due to weak charge of carboxyl latex. At pH > 7, zirconia has negative charge and we suppose that the deposition does not occur because of electrostatic repulsion between colloidal particles and collectors. The estimation of β=0.44/θ_{max} provides the information on the excluded area and the maximum surface coverage of the deposited particles on the collector surface.

The boundary conditions used in this study were

$$C = C_0 \text{ at } x = 0 \tag{28}$$

$$\frac{\partial C}{\partial x} = 0 \text{ at } x = L \tag{29}$$

and the initial conditions were

$$C = 0 \text{ for } 0 \le x \le L \text{ at } t \le 0 \tag{30}$$

$$\theta = 0 \text{ for } 0 \le x \le L \text{ at } t \le 0\,. \tag{31}$$

(3) Maximum surface coverage

The maximum surface coverage θ_{max} is 0.91 for the regular hexagonal packing of hard spheres deposited on the planar surface. However, the realization of such regular packing is not plausible in real situations. Instead, the random adsorption (RSA) model is available for the analysis of θ_{max}. In the RSA model, particles deposit randomly on the collector and the maximum surface coverage θ_{RSA} is around 0.55 [7),12),16)].

In the deposition of colloidal particles, the lateral electrostatic repulsion prevents the depositing particle to be placed near previously deposited particles. Therefore, θ_{max} decreases with increasing the lateral repulsive force. In the absence of hydrodynamic interaction, the explicit equation taking account of the surface potential of colloidal particles is available as follows[8),26)]:

$$\theta_{max} = \theta_{RSA}\frac{\left(1+N_R\right)^2}{\left(1+H^*\right)^2} \tag{32}$$

$$H^* = \frac{1}{\kappa a_p}\left[\ln\left(\xi\right) - \ln\left(1+\frac{1}{2\kappa a_p}\ln\left(\xi\right)\right)\right] \tag{33}$$

$$\xi = \frac{4\varepsilon_r\varepsilon_0 k_B T a_p}{10e^2}\tanh^2\left(\frac{e\psi_0}{k_B T}\right) \tag{34}$$

This expression indicates that θ_{max} is influenced by lateral electrostatic interaction controlled by the surface potential of the colloidal particle, and the attractive interaction between the colloidal particle and the collector is negligible for determining θ_{max}. In the adsorption of dendritic polyelectrolytes, however, the charge of substrate/collector affects the maximum surface coverage[13),14)]. To confirm the effect of collector charge on θ_{max} in colloid transport in porous media, we need experiments as carried out in this study.

4. RESULTS AND DISCUSSION

(1) Charging behavior

In **Fig. 2**, experimentally obtained electrophoretic mobilities of colloidal particles are plotted against pH. The data were taken in 1 mM KCl for carboxyl latex and colloidal zirconia and in 10 mM for sulfate

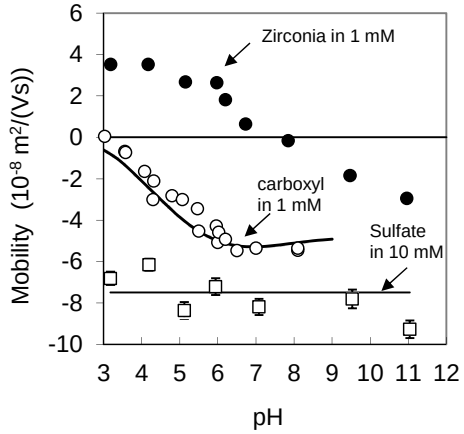

Fig.2 Electrophoretic mobility of colloidal particles against pH in KCl solution. Symbols and lines denote experimental data and theoretical calculation, respectively.

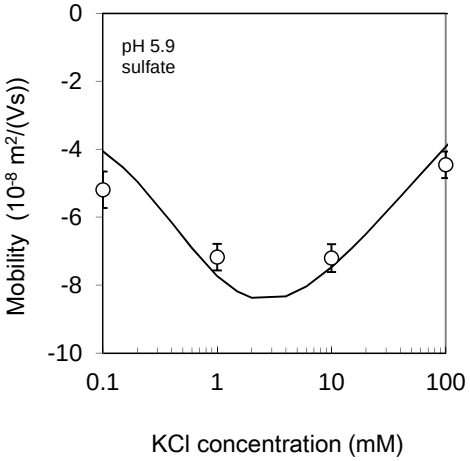

Fig. 3 Electrophoretic mobility of sulfate latex particles against KCl concentration. Symbols and lines denote experimental data and theoretical calculation, respectively.

latex. The mobility values of zirconia are positive at pH <7 and negative at pH > 7; the zirconia has the isoelectric point of pH 7. On the one hand, the mobility of the carboxyl latex is pH-dependent negative and shows the minimum. The appearance of the mobility minimum demonstrates the existence of the relaxation/polarization of the diffuse double layer[9),10),19),20)]. The mobility of sulfate is negative and almost the constant irrespective of pH. From these charging behaviors, we can expect the attractive electric double layer force between zirconia and latex at pH below 7. The dependence of the mobility of sulfate latex on KCl concentration is shown in **Fig. 3**. The mobility shows the minimum at KCl concentrations between 1 and 10 mM, indicating the significant effect of the double layer relaxation[6),17),27)]. Therefore, the mobility of our particles is influenced by the deformation or relaxation of the diffuse double layer. Thus, the Smoluchowski equation is no longer valid. Instead, the theory taking into account the relaxation, like Ohshima's equation, Eqs. (1) and (2) must be used.

The lines in **Figs. 2** and **3** are drawn by the mobility equation by Ohshima and the charging model described in Sec. 3 (1). In the calculation of the mobility of the carboxyl latex, parameters pK = 4.9, Γ_T = 0.52 /nm^2, and x_s = 0.25 nm are used. The values of pK and x_s are identical to those used in the previous studies[9),10)]. The site density Γ_T is here a fit value and is in reasonable range compared to that used so far[9),10)]. As for the sulfate latex, x_s = 0.25 nm and σ = -0.084 C/m^2 are adopted. As can be seen in **Figs. 2** and **3**, the calculated mobility shows good agreement with the experimental data. Therefore, we can now evaluate the charging characteristic, the surface potential and the surface charge density, of the colloidal particles by using the charging model in Sec. 3 (1). The calculated values of surface potential are available for the evaluation of the maximum surface coverage under the influence of the lateral electrostatic repulsion between colloidal particles deposited on the collector using Eqs. (32), (33), (34) .

(2) Colloid transport and the maximum surface coverage

Figs. 4-9 show typical breakthrough curves of latex particles leaked from the packed bed of zirconia. **Figs. 4, 5, 6,** and **9** show the data for carboxyl latex, and **Figs. 7** and **8** are for the sulfate latex. The data in each graph were taken at different pH. From these figures, one can realize the significant influence of pH on the transport of carboxyl latex in porous media. Note that the range of the abscissa is narrow in **Fig. 4**.

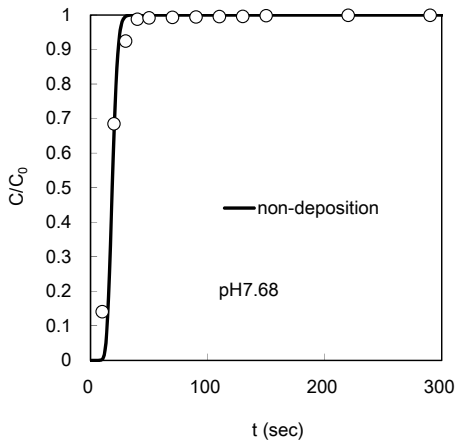

Fig. 4 Breakthrough curve of carboxyl latex at pH 7.68. Symbols are experimental data. Line is drawn by assuming that no deposition occurs α_{pp} =0 and α_{pc} =0.

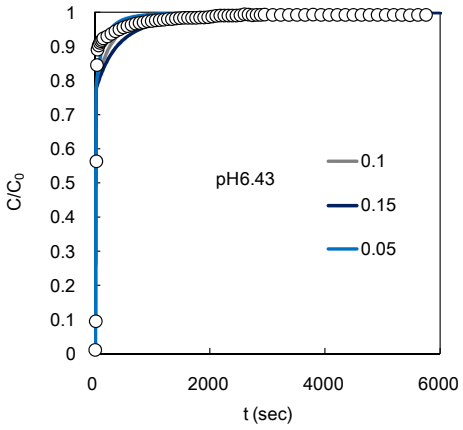

Fig. 5 Breakthrough curve of carboxyl latex at pH 6.43. Symbols are experimental data. Lines are theoretically drawn by assuming α_{pp} =0 and α_{pc} =1. Numbers in the figure indicate the blocking parameter, 1/β.

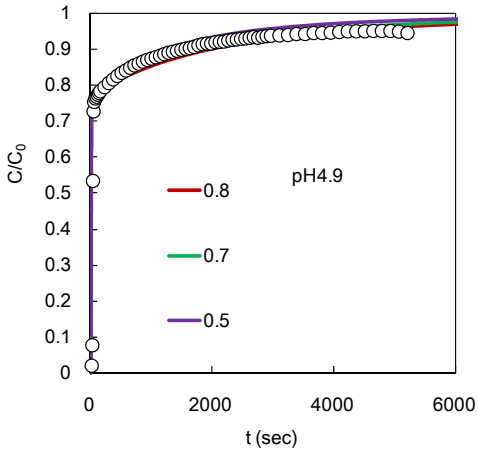

Fig. 6 Breakthrough curve of carboxyl latex at pH 4.9. Symbols are experimental data. Lines are theoretically drawn by assuming α_{pp} =0 and α_{pc} =1. Numbers in the figure indicate the blocking parameter, 1/β.

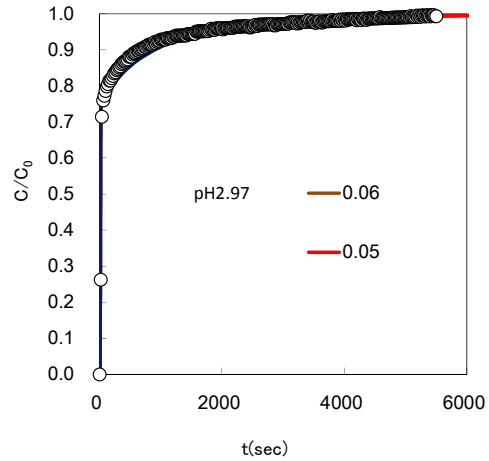

Fig. 7 Breakthrough curve of sulfate latex at pH 2.97. Symbols are experimental data. Lines are theoretically drawn by assuming α_{pp} =0 and α_{pc} =1. Numbers in the figure indicate the blocking parameter, $1/\beta$.

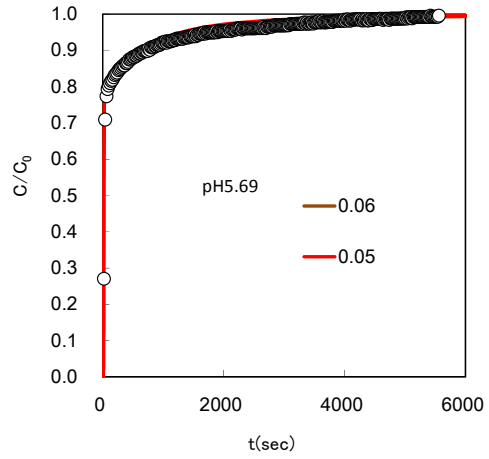

Fig. 8 Breakthrough curve of sulfate latex at pH 5.69. Symbols are experimental data. Lines are theoretically drawn by assuming α_{pp} =0 and α_{pc} =1. Numbers in the figure indicate the blocking parameter, $1/\beta$.

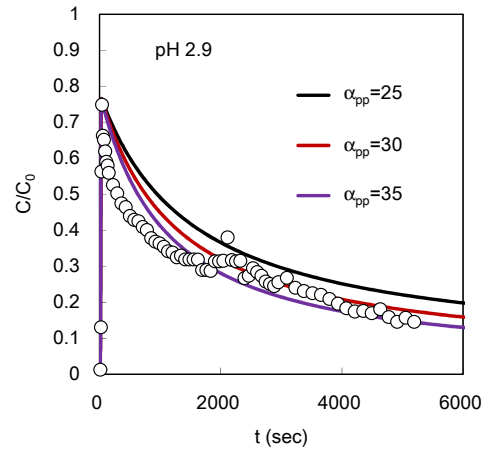

Fig. 9 Breakthrough curve of carboxyl latex at pH 2.9. Symbols are experimental data showing ripening behavior. Lines are theoretically drawn by assuming $1/\beta$=1.24 (θ_{max}=0.547) and α_{pc} =1.

Fig. 4 shows that the effluent concentration C rapidly rises and the C/C_0 becomes larger than 0.99 within 50 s and reaches unity, demonstrating that no deposition occurred. At pH > 7, both the zirconia and the carboxyl latex are negatively charged and thus the electrostatic repulsion prevents the deposition of carboxyl latex on the zirconia collector. As a consequence, the theoretical curve by Eq. (17) with the assumption of no-deposition α_{pp}=α_{pc}=0 captures the experimental data.

Figs. 5, 6, 7, and **8** show a similar shape of breakthrough curves; the C/C_0 increases with time and finally reaches unity. The curve reflects the blocking behavior. That is, in the early stage, the colloidal particles are deposited onto the collector beads. Therefore, the C/C_0 is below unity because of the reduction of C. As the deposition proceeds, the previously deposited particle interrupts the further deposition. Once the collector surface is sufficiently covered by attached particles, the deposition no longer occurs. This results in the gain of C/C_0 to unity. Theoretical curves in **Figs. 5, 6, 7,** and **8** are calculated by Eq. (17) with the parameters α_{pp}=0, α_{pc}=1, and various values of $1/\beta$. From the fit value of $1/\beta$, θ_{max} was determined at each pH and the values are plotted against pH in **Fig. 10**. Meaning of α_{pp}=0 and α_{pc}=1 is that both the multiple deposition and the significant enhancement of deposition rate by electrostatic attraction are not effective as mentioned above. That is, electrostatic repulsion between colloidal particles prevents aggregation and thus multiple deposition is negligible (α_{pp} =0). Also, the van der Waals force is dominant as physicochemical force (α_{pc}=1). In these situations, monolayer of deposited particles is formed as shown in **Fig. 11 a)**, where the distance between particles is affected by the lateral interaction of colloidal particles.

The breakthrough curve of carboxyl latex at low pH shown in **Fig. 9** is quite different. This figure indicates the occurrence of ripening behavior[2]. At low pH, the repulsive force between carboxyl latex particles weakens and thus the multiple deposition happens as shown in **Fig. 11 b)**. The dendritic structure formed by the multiple deposition of particles effectively captures the next coming particle due to the physical enmeshing and increased surface area. As a result, the C/C_0 gradually reduces to lower values. Theoretical curves qualitatively describe this behavior by using α_{pc}=1, very high values of α_{pp}, and $1/\beta$=0.547/0.44=1.24 corresponding to the saturated θ_{max} based on the RSA model. The assumption of $1/\beta$=1.24 is because the lateral repulsive force between carboxyl latex particles at low pH becomes so weak that the particles can deposit at closely packed configuration. As for α_{pp}, higher values of α_{pp}~30

probably reflect the physical enmeshing and the increased surface area provided by the dendritic structure formed by the layer of multiply deposited particles[2] as illustrated in **Fig. 11 b)**. However, the unambiguous evaluation of α_{pp} is difficult at this moment.

Symbols in **Fig. 10** are the experimentally determined θ_{max} from the fit of Eq. (17). While the θ_{max} of the sulfate latex is constant, that of carboxyl latex decreases with pH. Since the positive charge of zirconia increases at low pH, one may expect the increase of θ_{max} at low pH due to the strong attraction between highly charged zirconia and oppositely charged sulfate latex as found for the deposition of dendritic polyelectrolyte with nanometer size[14]. Nevertheless, the expected pH-dependence is not observed for the sulfate latex. This result suggests that the lateral repulsive interaction between colloidal particles is important, rather than the attractive particle-collector interaction as a controlling factor of θ_{max}. This suggestion is supported by the pH-dependent θ_{max} of the carboxyl latex; the tendency can be explained by the decrease of the lateral repulsion due to the loss of negative charge at low pH.

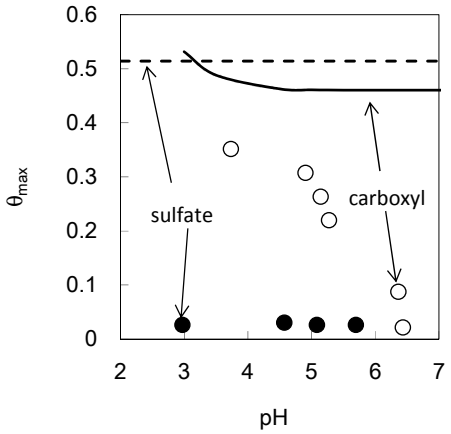

Fig. 10 Maximum surface coverage against pH. Symbols are experimental data. Lines are theoretically drawn by using charging parameters tuned by the analysis of measured electrophoretic mobility.

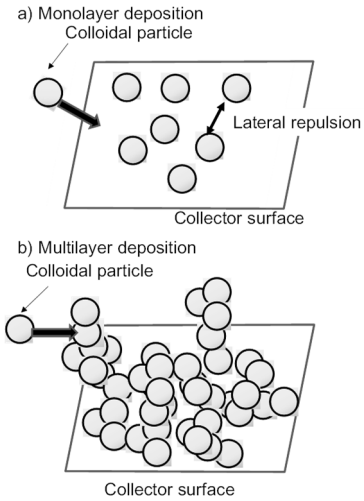

Fig. 11 Schematic illustrations of the collector surfaces covered with deposited particles: a) monolayer deposition for α_{pp}=0 . b) multilayer deposition for higher α_{pp}, where the dendritic structure formed by deposited particles effectively captures the colliding particle.

The lines in **Fig. 10** are evaluated by Eq. (32) with the surface potential estimated by the charging model using the tuned parameters. As shown in the figure, the calculated values are much higher than the experimental data. The RSA model with the lateral repulsive force successfully describes the θ_{max} for the deposition of nanoparticles[12),13),14)]. The success of the RSA is because the transport of nanoparticles is governed by Brownian diffusion; the diffusion controlled process matches the assumption in the RSA model. This study has used the micron-sized particles; the transport and particle-particle interaction are affected by hydrodynamic force. The effect of hydrodynamic interaction is illustrated in **Fig. 12**. That is, the colliding particle is hydrodynamically scattered by the previously deposited particle and cannot attach to the downstream area in the back of the deposited particle. Such area, where colloidal particles cannot attach, is called shadow area/region[8),16),28)]. The shadow area increases with increasing the particle size and with increasing the lateral repulsion between colloidal particles. Therefore, the values of the maximum surface coverage in this study are much lower than the prediction of the RSA model assuming random deposition. We need to develop theories that quantitatively predict the shadow area in the packed bed of granular materials as future studies.

In the present study, we first demonstrate that the solution pH, that is, the surface charge of colloidal particles, strongly affects the blocking and colloid transport in porous media. The electro-hydrodynamic scattering significantly changes the colloid transport phenomena in porous media. One has to keep in mind

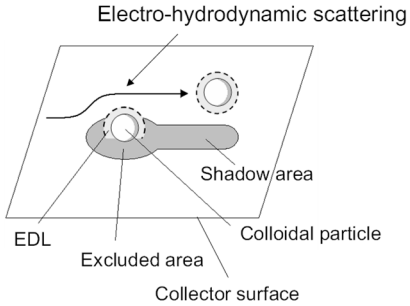

Fig. 12 Schematic representation showing the effect of electro-hydrodynamic interaction on the reduction of the maximum surface coverage. The depositing particles cannot deposit on the shadow area behind the deposited particle. EDL stands for electric double layer.

the surface charging and the size of colloidal particles are crucial factors when considering the transport process of colloidal particles in porous media.

5. CONCLUSIONS

We performed the experiment on the charging and transport of sulfate and carboxyl latex particles. The transport experiment was carried out in a packed bed of zirconia beads. The experiments were carried out as a function of pH to clarify the influence of surface charging on the colloid transport behavior in porous media. Experimentally obtained breakthrough curves were analyzed by the convection dispersion equation with the deposition of colloidal particles.

The results of experiments and analysis demonstrate that the maximum surface coverage of sulfate latex is constant irrespective of pH. On the one hand, the maximum coverage of carboxyl latex decreases with increasing pH, indicating that increased lateral particle-particle repulsion enhances the blocking in later stages of deposition. Electro-hydrodynamic interaction also reduces the maximum coverage.

ACKNOWLEDGMENT: The authors are grateful to the financial support from the JSPS KAKENHI (23688027).

REFERENCES

1) McCarthy, J. F., & McKay, L. D.: Colloid transport in the subsurface. *Vadose Zone Journal*, Vol. 3(2), pp. 326-337, 2004.
2) Kretzschmar, R., Borkovec, M., Grolimund, D., Elimelech, M: Mobile subsurface colloids and their role in contaminant transport, *Adv. Agronomy*, Vol. 66, pp. 121-193, 1999.
3) Elimelech, M., Jia, X., Gregory, J., & Williams, R.: *Particle deposition & aggregation: measurement, modelling and simulation*. Butterworth-Heinemann, 1998.
4) Nelson, K. E., & Ginn, T. R.: New collector efficiency equation for colloid filtration in both natural and engineered flow conditions. *Water Resources Research*, Vol. 47(5), 2011. DOI: 10.1029/2010WR009587.
5) Tufenkji, N., & Elimelech, M.: Correlation equation for predicting single-collector efficiency in physicochemical filtration in saturated porous media. *Environmental Science & Technology*, Vol. 38(2), pp. 529-536, 2004.
6) Kobayashi, M., Nanaumi, H., & Muto, Y.: Initial deposition rate of latex particles in the packed bed of zirconia beads. *Colloids and Surfaces A*, Vol. 347(1), pp. 2-7, 2009.
7) Kuhnen, F., Barmettler, K., Bhattacharjee, S., Elimelech, M., & Kretzschmar, R.: Transport of iron oxide colloids in packed quartz sand media: monolayer and multilayer deposition. *J. Colloid Interface Science*, Vol. 231(1), 32-41, 2000.
8) Ko, C. H., Bhattacharjee, S., & Elimelech, M.: Coupled influence of colloidal and hydrodynamic interactions on the RSA dynamic blocking function for particle deposition onto packed spherical collectors. *J. Colloid Interface Science*, Vol. 229(2), pp. 554-567, 2000.
9) Sugimoto, T., Kobayashi, M., & Adachi, Y.: The effect of double layer repulsion on the rate of turbulent and Brownian aggregation: experimental consideration. *Colloids and Surfaces A*, Vol. 443, 418-424, 2014.
10) Behrens, S. H., Christl, D. I., Emmerzael, R., Schurtenberger, P., & Borkovec, M.: Charging and aggregation properties of carboxyl latex particles: Experiments versus DLVO theory. *Langmuir*, Vol. 16(6), pp. 2566-2575, 2000.
11) Ottewill, R. H., & Shaw, J.: Stability of monodisperse polystyrene latex dispersions of various sizes. *Discuss. Faraday Soc.*, Vol. 42, pp. 154-163, 1966.
12) Kleimann, J., Lecoultre, G., Papastavrou, G., Jeanneret, S., Galletto, P., Koper, G. J., & Borkovec, M.: Deposition of nanosized latex particles onto silica and cellulose surfaces studied by optical reflectometry. *J. Colloid Interface Science*, Vol. 303(2), pp. 460-471, 2006.
13) Pericet-Camara, R., Cahill, B. P., Papastavrou, G., & Borkovec, M.: Nano-patterning of solid substrates by adsorbed dendrimers. *Chemical Communications*, Vol. 3, pp. 266-268, 2007.
14) Cahill, B. P., Papastavrou, G., Koper, G. J., & Borkovec, M.: Adsorption of poly (amido amine)(PAMAM) dendrimers on silica: Importance of electrostatic three-body attraction. *Langmuir*, Vol. (2), pp. 465-473, 2008.
15) Adamczyk, Z., Siwek, B., Zembala, M., & Weronski, P.: Kinetics of localized adsorption of colloid particles. *Langmuir*, Vol. 8(11), pp. 2605-2610, 1992.
16) Adamczyk, Z., Siwek, B., Zembala, M., & Belouschek, P.: Kinetics of localized adsorption of colloid particles. *Advances in Colloid Interface Science*, Vol. 48, pp. 151-280, 1994.
17) Kobayashi, M.: Electrophoretic mobility of latex spheres in the presence of divalent ions: experiments and modeling. *Colloid Polymer Science*, Vol. 286(8-9), pp. 935-940, 2008.
18) Kobayashi, M., Nitanai, M., Satta, N., & Adachi, Y.: Coagulation and charging of latex particles in the presence of imogolite. *Colloids and Surfaces A*, Vol. 435, pp. 139-146, 2013.
19) Ohshima, H., Healy, T. W., & White, L. R.: Approximate analytic expressions for the electrophoretic mobility of spherical colloidal particles and the conductivity of their dilute suspensions. *J. Chemical Society, Faraday Transactions* 2, Vol. 79(11), pp. 1613-1628, 1983.
20) Ohshima, H., & Furusawa, K. (Eds.): *Electrical Phenomena at Interfaces: Fundamentals: Measurements, and Applications*. CRC Press. 1998.
21) Lide, R. L.: *CRC Handbook in Chemistry and Physics*, 82nd. ed., CRC Press, 2001
22) Kobayashi, M.: Kinetics of shear coagulation of oppositely charged particles: A trajectory analysis. *Theoretical Applied Mechanics Japan*, Vol. 56, pp. 267-272, 2008.
23) Kobayashi, M.: Aggregation of unequal-sized and oppositely charged colloidal particles in a shear flow. *J. Applied Mechanics, JSCE*, Vol.11, pp. 517-523, 2008.
24) Sato, D., Kobayashi, M., & Adachi, Y.: Capture efficiency and coagulation rate of polystyrene latex particles in a laminar shear flow: Effects of ionic strength and shear rate. *Colloids and Surfaces A*, Vol. 266(1), pp. 150-154. 2005.
25) Kobayashi, M., Maekita, T., Adachi, Y., & Sasaki, H.: Colloid stability and coagulation rate of polystyrene latex particles in a turbulent flow. *International J. Mineral Processing*, Vol. 73(2), pp. 177-181, 2004.
26) Adamczyk, Z., & Belouschek, P.: Localized adsorption of particles on spherical and cylindrical interfaces. *J. Colloid Interface Science*, Vol. 146(1), pp. 123-136, 1991.
27) Chassagne, C., & Ibanez, M.: Electrophoretic mobility of latex nanospheres in electrolytes: Experimental challenges. *Pure and Applied Chemistry*, Vol. 85(1), pp. 41-51, 2012.
28) Ko, C. H., & Elimelech, M.: The "shadow effect" in colloid transport and deposition dynamics in granular porous media: measurements and mechanisms. *Environmental Science & Technology*, Vol. 34(17), pp. 3681-3689, 2000.

(Received June 20, 2014)